Preparation and Characterization of Poly(styrene butylacrylate) Latex/Nano-ZnO Nanocomposites

Mingna Xiong, Guangxin Gu, Bo You, Limin Wu

Department of Materials Science, Fudan University, Shanghai 200433, P. R. China

Received 15 August 2002; accepted 30 January 2003

ABSTRACT: Poly(styrene butylacrylate) latex/nano-ZnO composites were prepared by blending poly(styrene butylacrylate) latex with a water slurry of nano-ZnO particles, and the effects of certain parameters, such as particle size, dispersant type, dispersing time and others, on the dispersibility, mechanical properties, ultraviolet (UV) shielding and near infrared (NIR) shielding were investigated with transmission electron microscopy (TEM), an Instron testing machine, dynamic mechanical analysis and ultraviolet-visible-near infrared (UV-VIS-NIR) spectrophotometry. TEM observation showed that dispersants with long chains are better than those with short chains at enhancing the dispersibility of nano-ZnO particles in a matrix; extending dispersing time also improves the dispersibility of nano-ZnO particles in a matrix. Instron tests showed that the nanocomposite polymers embedded with nano-ZnO particles had much higher tensile strength than the corresponding composite polymers with micro-ZnO particles. As the nano-ZnO content increased, the temperature of glass transition (T_g) of the nanocomposite polymer embedded with 60 nm ZnO particles first increased then decreased, but 100 nm ZnO and micro-ZnO particles seemed to have no influence on the T_g of the composite polymers. The better dispersibility of nano-ZnO particles resulted in higher T_g values. Increasing nano-ZnO content or dispersibility could enhance the UV shielding properties of the nanocomposite polymers, and 60 nm ZnO particles could more effectively shield UV rays than 100 nm ZnO particles. Micro-ZnO particles basically had no effect on the UV absorbance of the composite polymers. A blue-shift phenomenon was observed at 365 nm when nano-ZnO particles were present in the nanocomposite polymers. NIR analysis indicated that as nano-ZnO content increased, the NIR shielding of the nanocomposite polymers increased, but the NIR shielding properties seemed to be more influenced by particle size than by the nano-effect. J Appl Polym Sci 90: 1923–1931, 2003

Key words: polystyrene; nanocomposites; coatings

INTRODUCTION

Nano-ZnO, as one of the multifunctional inorganic nanoparticles, has drawn increasing attention in recent years due to its many significant physical and chemical properties, such as high chemical stability, low dielectric constant, large electromechanical coupling coefficient, high luminous transmittance, high catalysis activity, intensive ultraviolet and infrared absorption, etc. Therefore, nano-ZnO can potentially be applied to catalysts, gas sensors, semiconductors, varistors, piezoelectric devices, field-emission displays and UV-shielding materials.[1–11] The introduction of nano-ZnO into polymers could improve the mechanical and optical properties of the polymers due to a strong interfacial interaction between the organic polymer and the inorganic nanoparticles and nanoparticle's small size and large specific area, and quantum effect, respectively. Consequently, these nanocomposites could be widely applied in coatings, rubbers, plastics, sealants, fibers and other applications.[1,12-13]

Correspondence to: L. Wu (lxw@fudan.ac.cn).

Journal of Applied Polymer Science, Vol. 90, 1923–1931 (2003)

In this article, poly(styrene butylacrylate) latex/ZnO nanocomposites were prepared, and the mechanical and optical properties of the composite polymers were investigated by transmission electron microscopy (TEM), an Instron testing machine, dynamic mechanical analysis (DMA), and ultraviolet-visible-near infrared (UV-VIS-NIR) spectrophotometry.

EXPERIMENTAL

Materials

Butylacrylate (BA, 96%), styrene (St, 97%) and acrylic acid (AA, 98%) were purchased from Shanghai Gaoqiao Petrochemical Company (China). The anionic surfactant (PHODAPEX CO436) – polyoxyethyene alkyl phenyl ether ammonium sulfate (moles of ethylene oxide (EO) = 4) and the nonionic surfactant (IGEPAL CA897) – polyoxyethyene octyl phenyl ether (moles of EO = 40) were supplied by Phone-Poulenc, Inc. (France). Ammonium persulfate and sodium bicarbonate were purchased from the Shanghai Chemistry Reagent Company. Dispersant A, Disperbyk-190®, an ultra-high molecular weight block copolymer with a strong anionic group, and dispersant B, polyacrylate sodium, were obtained from the BYK Com-

TABLE I
Synthesis of Poly(styrene butylacrylate) Latex

Ingredients		Weight (g)
Part A	BA	9.0
	St	21.0
	AA	4.0
	PAA	3.0
	CO436	2.0
	CA897	4.0
	H_2O	70.0
Part B	$NaHCO_3$	0.4
	$(NH_4)_2S_2O_8$	1.0
	H_2O	50.0
Part C	BA	82.0
	St	46.0
	CA897	1.2
	H_2O	70.0
Part D	$NaHCO_3$	0.2
	$(NH_4)_2S_2O_8$	1.2
	H_2O	70.0

pany of Germany and the Shanghai Wulian Chemical Company of China, respectively. All of the ingredients were used as received. Nano-ZnO particles with a mean size of 60 nm (specific area of 30 m^2/g) and 100 nm (specific area of 10 m^2/g) were purchased from Jiangshu Wuling Changtai Nanometer Materials Co., Ltd. of China. Micro-ZnO particles were the product of Shanghai Coating Co., Ltd. of China.

Synthesis of poly(styrene butylacrylate) latex

Synthesis of poly(styrene butylacrylate) latex (labeled as PURE) was carried out in a 500 mL four-necked round bottomed flask equipped with a heat mantle, mechanical stirrer, addition funnel and thermometer. The components of the latex are listed in Table I. The monomers, surfactant and deionized water, as indicated by Part A in Table I, were charged into the flask and heated to 60°C, after which the mixture of initiator and buffer solution was added, as shown by Part B. The materials were heated to 70 ± 2°C within 30 min with stirring to obtain seed latex. The pre-emulsified residual monomers, surfactants and deionized water, listed in Part C, and the mixture of initiator and buffer solution, listed in Part D, were added to the seed latex over a period of 2.0 h using an addition funnel and a constant flow pump, respectively, at 70°C. After the addition of all ingredients, the reaction mixture was maintained at 75°C for one additional hour to complete the reaction of residual monomers.[14]

Preparation of poly(styrene butylacrylate) latex/ nano-ZnO composites

A series of poly(styrene butylacrylate) latex / nano-ZnO composites were prepared by blending poly(styrene butylacrylate) latex with a water slurry of nano-ZnO particles under high shear stirring. The slurry was obtained through the ball milling method, and the processing parameters are summarized in Table II. The poly(styrene butylacrylate) latex/micro-ZnO composites were also prepared by the ball milling method for the sake of comparison.

Preparation of polymer films

The polymer films were prepared by casting pure poly(styrene butylacrylate) latex and poly(styrene butylacrylate) latex/nano-ZnO composite onto substrates that were then dried at room temperature for 20 days prior to TEM observation, DMA determination and tensile tests. The polymer films for the UV-VIS-NIR spectra experiments were prepared by casting latex onto glass panels and drying them at room temperature for 5 days. The thickness of the films was controlled within 64–68 μm.

Transmission electron microscopy (TEM)

TEM micrographs of the water slurry of nano-ZnO particles and the composite polymer films were carried out in a Hitachi H-600 apparatus (Hitachi Corporation, Japan). TEM micrographs of the water slurry of nano-ZnO particles were determined on copper girds directly, and the samples obtained from the composite polymer films were prepared by ultramicrotomy at 25°C, giving sections of nearly 100 nm in thickness. No further staining was used to improve contrast.

Static mechanical properties

Tensile properties were determined by an Instron model DXLL 1000-20000 testing machine (Shanghai,

TABLE II
Processing Parameters for Preparation of Poly(styrene butylacrylate) Latex/Nano-ZnO Composites

Labels	Type of dispersant	Size of ZnO particles	Time of ball milling	Content of ZnO particles
A1	A	60 nm	4 h	3 wt %
	A	60 nm	4 h	5 wt %
	A	60 nm	4 h	7 wt %
	A	60 nm	4 h	9 wt %
A2	A	100 nm	4 h	3 wt %
	A	100 nm	4 h	5 wt %
	A	100 nm	4 h	7 wt %
	A	100 nm	4 h	9 wt %
A3	A	μm	4 h	3 wt %
	A	μm	4 h	5 wt %
	A	μm	4 h	7 wt %
	A	μm	4 h	9 wt %
B1	B	60 nm	4 h	5 wt %
B2	B	60 nm	1 h	5 wt %
B3	B	60 nm	0.5 h	5 wt %

China). The specimens for the tensile tests were dumbbell cut from the molded polymer films according to Die C of ASTM-D412 and carried out at a crosshead speed of 200 mm/min and a temperature of 23 ± 2°C. A 20 mm benchmark and the original cross-sectional area were utilized to calculate tensile properties. The ultimate tensile strength and elongation were automatically calculated by the computer connected to the Instron. The average of at least five measurements for each sample was reported, and the experimental error was ±10%.

FTIR analysis

Nano-ZnO particles were dried at 100°C for 3 h and dispersed in KBr powder for FTIR analysis by a Magna-IR™ 550 spectrometer (Nicolet Instruments, Madison, WI).

Dynamic mechanical analysis (DMA)

Dynamic mechanical measurements were carried out on a DMA242 (Netzsch Inc., German). The samples were quickly cooled to −50°C and equilibrated for 3 min at that temperature and then heated to 100°C at a frequency of 1 Hz with a constant heating rate of 5°C/min under nitrogen atmosphere.

UV-VIS-NIR spectra

The UV-VIS-NIR spectra of the polymer films were carried out on an UV-VIS-NIR spectrophotometer (Lambda 900, Perkin-Elmer Company). The absorbance and transmittance spectra were determined in air, while the scattering spectra were tested on an integral ball with a diameter of 150 mm. The scan speed was 300 nm/min in the range of 200–2000 nm wavelength light.

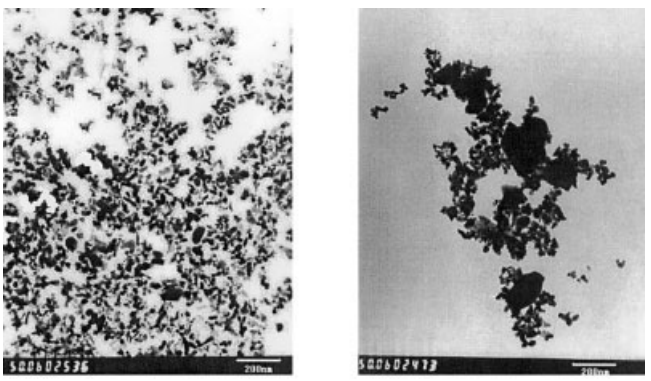

Figure 1 TEM micrographs of 60 nm nano-ZnO particles dispersed into water with (a) dispersant A, (b) and dispersant B.

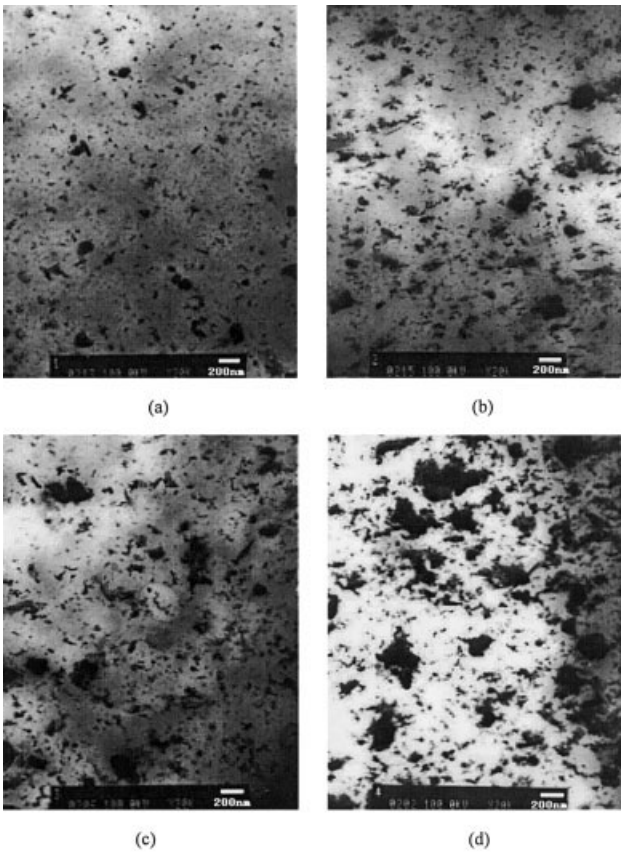

Figure 2 TEM micrographs of A1 series composites with nano-ZnO contents of (a) 3 wt %, (b) 5 wt %, (c) 7 wt % and (d) 9 wt %.

RESULTS AND DISCUSSION

Dispersion of nano-ZnO particles and morphology of composite polymers

Two types of dispersants were used in the preparation of the water slurry of nano-ZnO particles through the ball milling method. Figure 1 presents the TEM micrographs of 60 nm nano-ZnO particles dispersed into water via ball milling for 4 h. During the addition of dispersant A, almost all ZnO nanoparticles were dispersed into the original size, as indicated by Figure 1(a), but when dispersant B was used, although a considerable number of nano-ZnO particles were dispersed to nano-scale, some agglomerates of ZnO nanoparticles with sizes of 200–300 nm were observed, as shown in Figure 1(b). Recall that dispersant A is an ultra high molecular weight block polymer and has a strong affinity for pigments, while dispersant B is polyacrylate sodium with a molecular weight of only several thousand. This suggests that the chain length of the dispersant could improve the dispersibility of nano-ZnO particles into water due to steric and static stabilization effects.

Figure 2 illustrats the TEM micrographs of the A1 series of poly(styrene butylacrylate) latex/nano-ZnO

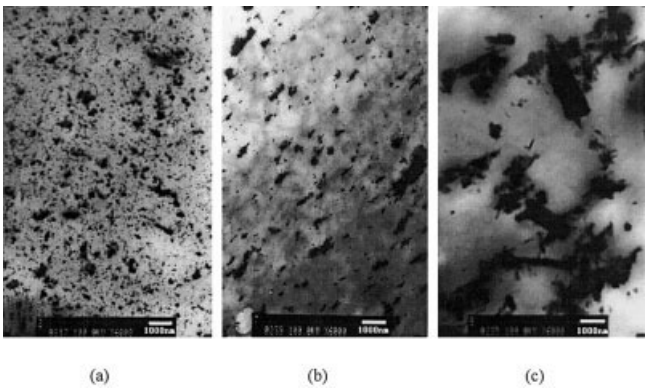

Figure 3 TEM micrographs of composites with 5 wt % ZnO particles of size (a) 60 nm, (b) 100 nm and (c) 1 μm.

composites with various nano-ZnO contents. The dispersibility of the nanoparticles in the composites decreased with increasing nano-ZnO content. Almost all of the nanoparticles inside the nanocomposite with 3 wt % ZnO content were dispersed to nano-scale, as shown in Figure 2(a). As more nano-ZnO particles were used, more nano-ZnO agglomerates were observed, as shown in Figure 2(b-d). Figure 3 further compares the dispersibility of different ZnO particles in the composites with the same ZnO content. For sample A1 with nano-ZnO particles of 60 nm in size, the nanoparticles were dispersed almost to the nano-scale. When the nano-ZnO particles of 100 nm in size were embedded in the composite, although nano-scale ZnO particles were obtained, some ZnO agglomerates were also observed.

The effect of nano-ZnO dispersing time in water on the dispersibility of the nanocomposites is shown in Figure 4, which presents the TEM micrographs of the nanocomposites containing 5 wt % 60 nm nano-ZnO particles and dispersant B. As the dispersing time of nano-ZnO in water increased, the dispersibility of nano-ZnO particles in the composites increased. Comparing Figure 4(a) and Figure 3(a), with dispersants B and A, respectively, further confirms that long chain

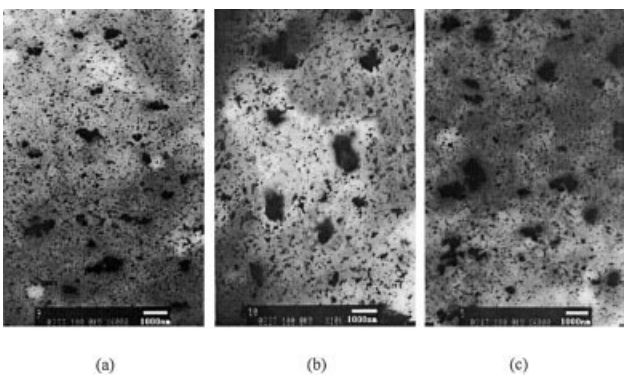

Figure 4 TEM micrographs of samples with 5 wt % ZnO content: (a) B1, (b) B2 and (c) B3.

TABLE III
Mechanical Properties of PURE, A1, A2 and A3 Samples

Samples	Content ZnO	Tensile strength (MPa)	Elongation at break (%)
PURE	0 wt %	2.30	448.4
A1	3 wt %	4.63	374.5
	5 wt %	4.83	390.6
	7 wt %	4.95	389.9
	9 wt %	5.04	385.8
A2	3 wt %	4.96	369.2
	5 wt %	5.03	367.5
	7 wt %	5.18	371.9
	9 wt %	5.33	389.9
A3	3 wt %	3.54	394.8
	5 wt %	4.13	387.6
	7 wt %	4.30	388.2
	9 wt %	4.57	377.2

dispersant favors the dispersion of nano-ZnO particles in a medium, as discussed above.

Tensile properties of composite polymer films

The tensile properties of the polymer films obtained from the three series composite latex (A1, A2 and A3 series) were determined with an Instron testing machine. Table III summarizes the experimental results. As expected, the polymers embedded with nano-ZnO particles (A1 and A2 series) show much higher tensile strength than the polymers filled with micro-ZnO particles (A3 series), since nanoparticles have much larger surface area than micro particles of the same weight, which results in the nanoparticles having stronger interfacial interaction with polymer molecules. It was a little surprising that the polymers embedded with 100 nm ZnO particles had higher tensile strength than the polymers embedded with 60 nm ZnO particles because 60 nm ZnO particles theoretically have more surface area than 100 nm ZnO particles. To explore this result, FTIR spectra of 60 nm and 100 nm ZnO particles were taken and are shown in Figure 5. Both

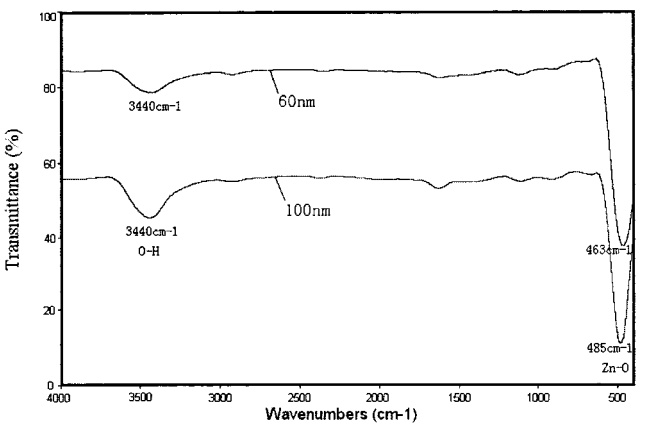

Figure 5 FTIR spectra of nano-ZnO powders.

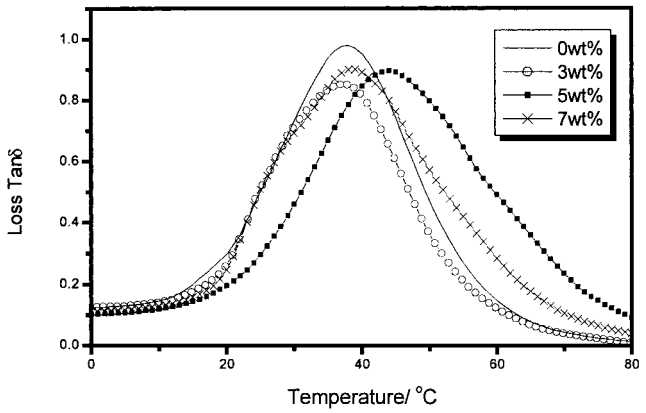

Figure 6 Loss tangent curves of polymers obtained from A1 series composites.

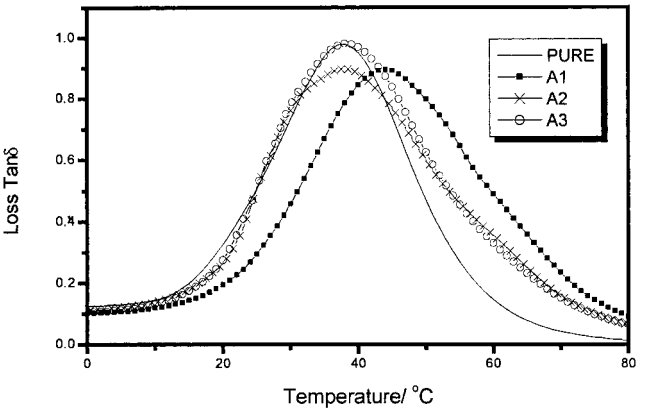

Figure 7 Loss tangent curves of polymers from composites with 60 nm, 100 nm and 1 μm ZnO particle size at 5 wt % ZnO content.

sizes of ZnO nanoparticles showed an absorption peak at 3440 cm^{-1} due to the presence of OH groups, as well as absorption peaks at 463 cm^{-1} and 485 cm^{-1}, assigned to the Zn—O groups of 60 nm ZnO and 100 nm ZnO, respectively. The ratios of the OH absorption peak heights to the Zn—O bonding absorption peak heights, based on a curve-fitting technique and an iterative least-squares computer program, are 0.43 and 0.72 for 60 nm ZnO and 100 nm ZnO, respectively. This means that 100 nm ZnO particles have more OH groups at their surface, leading to stronger interfacial interaction between nanoparticles and the polymer matrix in comparison with 60 nm ZnO particles. This suggests that not only the small size effect, but also the surface group effect, influences the properties of polymers.

As ZnO content increased, the tensile strength of the nanocomposite polymers increased, while the elongation at break didn't change appreciably within our experimental range.

DMA of composite polymer films

The loss tangent, tanδ of the composite polymers as a function of temperature was determined by DMA and is displayed in Figures 6–8. The tanδ peaks at 37–44°C should be due to the micro-Brownian segmental motion of amorphous acrylic-styrene copolymer, which is assigned to the glass transition temperature (T_g) of styrene-butyl acrylic copolymer. As shown in Figure 6, the T_g values of the polymers from the A1 series nanocomposites increased first then decreased as the nano-ZnO content increased. The increase in T_g of the nanocomposite polymers could be attributed to the strong interfacial interaction between the nanoparticles and the polymer matrix, leading to a decrease in the free volume, which limits the motion of segmental chains. However, when the nano-ZnO content increased, agglomerates increased, as observed by TEM and shown in Figure 2. Correspondingly, the free volume of matrix surrounding these agglomerates enlarged, resulting in easy chain motion and the observed lowering of the T_g.

The effect of different sizes of ZnO particles in the composites on the tanδ values is illustrated in Figure 7. The composite polymers with 100 nm ZnO and micro-ZnO showed almost no change in T_g in comparison with pure polymer, as seen by curves A2 and A3, respectively, while the composite polymer embedded with 60 nm ZnO particles had an obvious increase in T_g. This is probably because the increased T_g caused by the small size effect and the surface group effect was counteracted by some agglomerates in the 100 nm ZnO containing film.

Figure 8 further presents the effect of nano-ZnO dispersibility in water on the tanδ of the composite polymers. The T_g values of the nanocomposite polymers obtained from B series composites were lower the values for A1 composites, and the T_g increased slightly as dispersing time was extended. This also

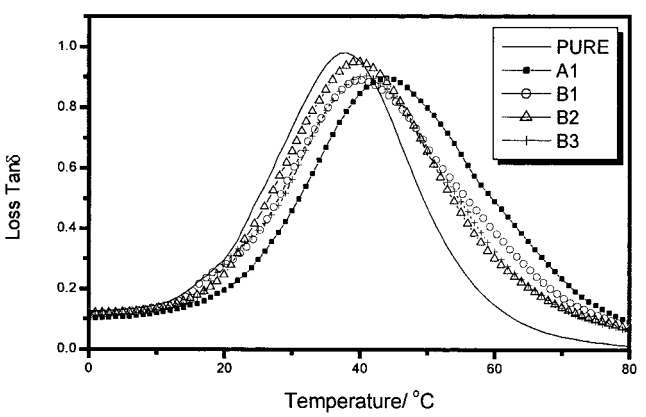

Figure 8 Loss tangent curves of polymers obtained from A1, B1, B2 and B3 nanocomposites with 5 wt % nano-ZnO content.

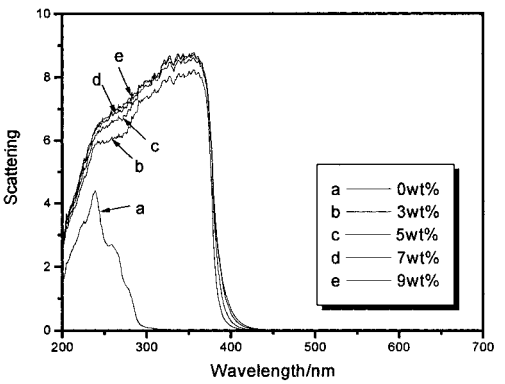

(a)

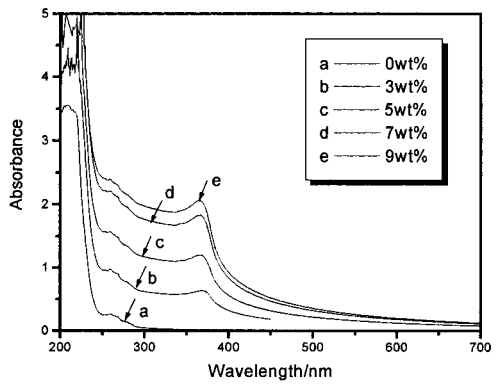

(b)

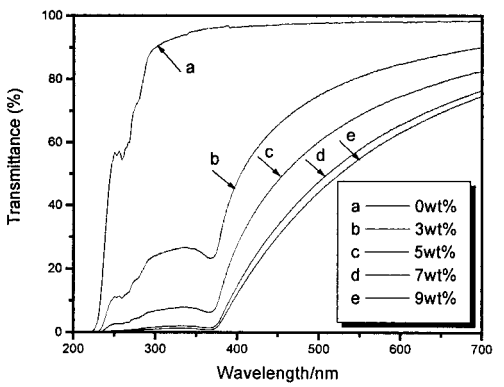

(c)

Figure 9 UV-VIS spectra of polymers obtained from A1 series composites: (a) scattering, (b) absorbance and (c) transmittance

suggests that an increase in dispersibility of nano-ZnO particles could enhance the T_g of the polymer matrix.

UV-VIS spectra

The ultraviolet-visible scattering, absorbance and transmittance spectra of the nanocomposite polymers obtained from A1 series composites with various contents of 60 nm ZnO particles are shown in Figure 9. The scattering is remarkably enhanced in the UV range (290–400 nm) with the addition of ZnO nanoparticles compared to scattering in the pure polymer, as demonstrated in Figure 9(a), and the scattering in the UV region increased slightly as the nano-ZnO content increased, owing to the increase in agglomerates indicated by TEM. The UV absorbance of the nanocomposite polymers also increased as the nano-ZnO content increased [see Fig. 9(b)], just as found in our previous studies.[14] Nevertheless, an absorption peak was found at 365 nm for the nanocomposite polymers, and the intensity of the peak increased with increasing nano-ZnO content. This is because the ZnO bulk material had a band-gap at around 3.3 eV (corresponding to 376 nm). The absorption peak at 365 nm for the polymers embedded with 60 nm ZnO indicated some blue-shift phenomenon due to the quantum size effect of nano-ZnO particles.[15–18] The transmittance of the nanocomposite polymers from the A1 series in the UV region is displayed in Figure 9(c). As the nano-ZnO content increased, the transmittance of UV light decreased. When the ZnO content reached 7%, almost all UV-rays were shielded.

The effect of different sizes of ZnO particles in the composites on the ultraviolet-visible scattering, absorbance and transmittance is demonstrated in Figure 10. Scattering for the nanocomposite polymers embedded with 60 nm and 100 nm ZnO particles is much higher than that of the pure polymer in the UV range [see curves A1 and A2 in Fig. 10(a)], while for the composite polymer filled with micro-ZnO particles, the scattering is nearly unchanged compared to the pure polymer [see curve A3 in Fig. 10(a)]. Moreover, nanocomposite polymers containing 60 nm ZnO particles have slightly higher UV scattering than those containing the same content of 100 nm ZnO particles. The result can be explained according to Scamatakis formula[19]:

$$S = [\alpha M^3(\lambda)^{1/2}]/[\lambda^2/2d + n_b^2\pi^2 Md]$$

where S is the scattering coefficient, α is a constant (related to the properties of the material), λ is the wavelength of incident light, n_p and n_b are the refractive index of the dispersed phase and the dispersed medium, respectively, and d is the diameter of particles. The value of M can be calculated by the following equation:

$$M = (n_p/n_b)^2 - (n_b/n_p)^2 + 2,$$

For this system, n_p is 1.90 and n_b is 1.55. For a certain wavelength of incident light, the maximum S value can be reached when d is equal to $\lambda/n_b\pi\sqrt{2M}$. Consequently, the diameter of particles for maximum scattering of UV-light (290–400 nm) is about 25–35 nm.

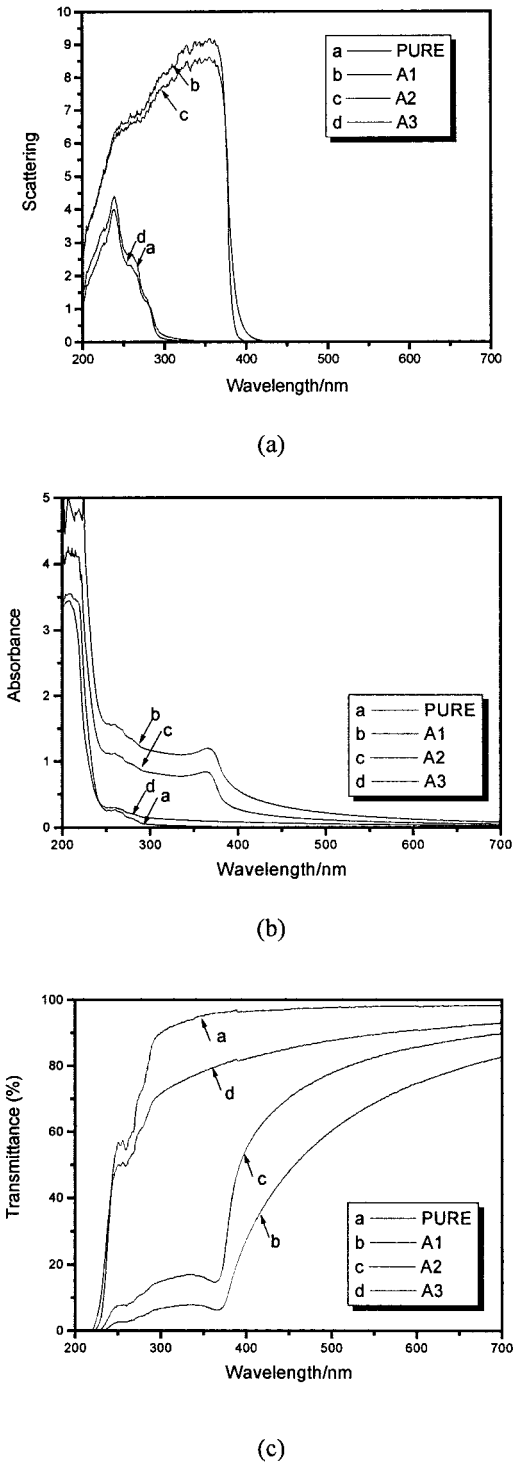

Figure 10 UV-VIS spectra of composite polymers with 60 nm, 100 nm and 1 μm ZnO particle size at 5 wt % ZnO content: (a) scattering, (b) absorbance and (c) transmittance.

The scattering decreased with the increasing particle size when the size was larger than 25–35 nm. Within the region, the same ZnO mass with smaller particle size had more particles than that with large particle size, which also leads to an increase in UV scattering.

The UV absorbance spectra of the nanocomposite polymers obtained from composites A1, A2 and A3, as well as that of the pure polymer, are shown in Figure 10(b). Nano-ZnO particles can increase the UV absorbance of the nanocomposite polymers, while micro-ZnO particles basically have no influence on UV absorbance, as shown by curves A1, A2 and A3 in Figure 10(b). The smaller the nano-ZnO particle size was, the

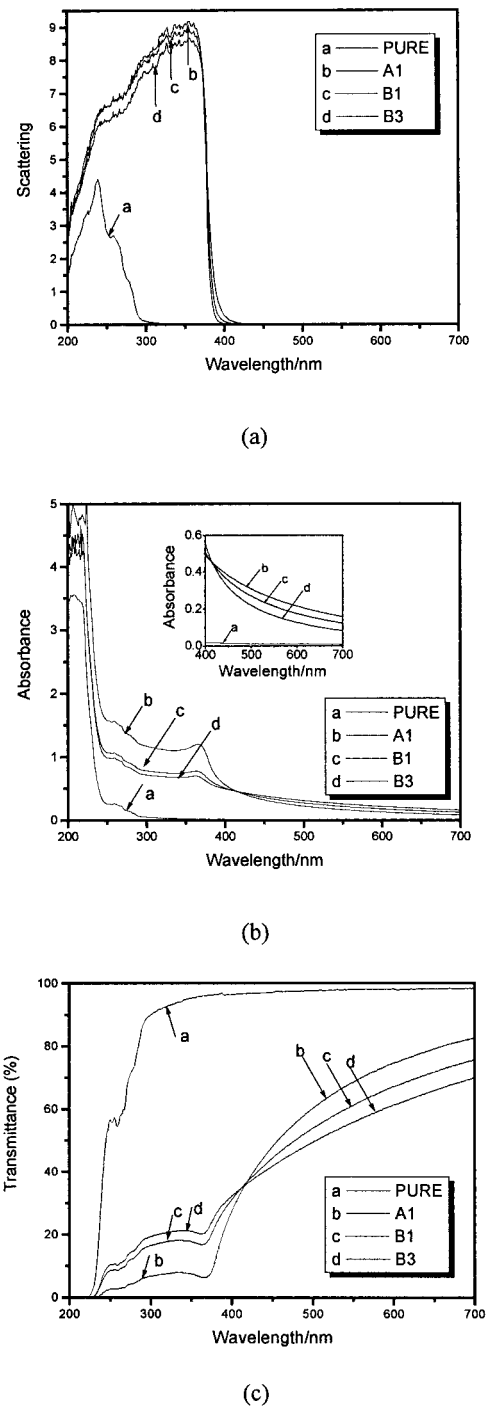

Figure 11 UV-VIS spectra of nanocomposite polymers from A1, B1 and B3 series with 5 wt % ZnO content: (a) scattering, (b) absorbance and (c) transmittance.

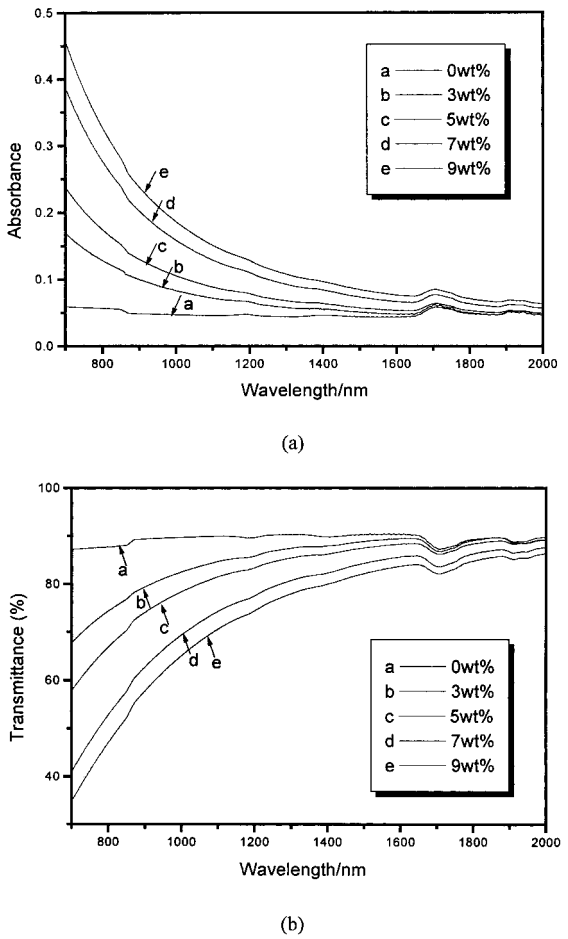

Figure 12 NIR spectra of polymers obtained from A1 series composites: (a) absorbance and (b) transmittance.

higher the UV absorbance of the nanocomposite polymer. Again, the absorption peak at 365 nm was observed for the nanocomposite polymers with 60 nm and 100 nm ZnO particles. Transmittance in the UV range for the composite polymers had the same changing trend as that seen in the UV scattering and absorbance, as indicated in Figure 10(c). This suggests that the nanocomposite polymers embedded with nano-ZnO have excellent UV-shielding properties, and the nanocomposite polymer with smaller nano-ZnO particles has even better UV-shielding properties.

Figure 11 further illustrates the influence of differing dispersibility of nano-ZnO particles on the ultraviolet-visible scattering, absorbance and transmittance of the nanocomposite polymers. It was found that the better the dispersibility of the nano-ZnO particles was, the better the scattering and absorbance of UV rays and the lower the transmittance of UV light. Nevertheless, the better transparent films were obtained due to the lower absorbance and higher transmittance of VIS-light. The absorbance intensity at 365 nm also increased as the dispersibility increased.

NIR spectra

The NIR absorbance and transmittance spectra were carried out in a Lambda 900 spectrophotometer. The NIR absorbance and transmittance of the nanocomposite polymers from the A1 series with various nano-ZnO contents are shown in Figure 12. As ZnO content increased, the absorbance increased and the transmittance decreased greatly in the range from 700–2000 nm (NIR region), especially between 700 and 1500 nm wavelength.

Figure 13 demonstrates the NIR absorbance and transmittance spectra for the composite polymers with different ZnO particles at the same content. No matter which size of ZnO particles was dispersed into the polymer, the absorbance and transmittance of the composite polymers in the NIR range were remarkably increased and decreased, respectively, compared with the pure polymer. Comparing the three composite polymers showed that nano-ZnO particles had no obvious superiority over micro-ZnO particles in NIR absorbance and transmittance. The influence of differing dispersibility of ZnO nanoparticles on the near

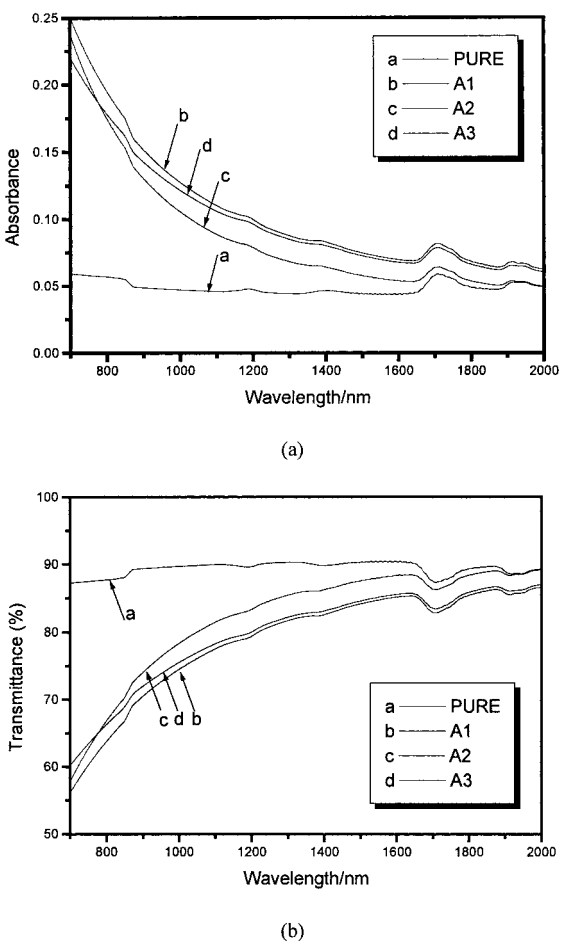

Figure 13 NIR spectra of composite polymers with 60 nm, 100 nm, and 1 μm ZnO particle size at 5 wt % ZnO content: (a) absorbance and (b) transmittance.

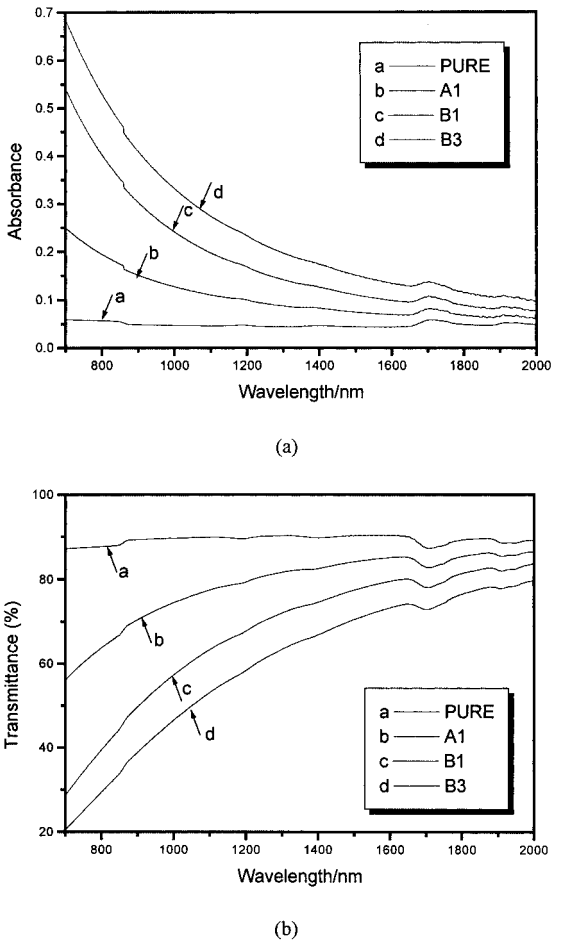

Figure 14 Spectra of nanocomposite polymers from A1, B1 and B3 series with 5 wt % ZnO content: (a) absorbance and (b) transmittance.

infrared absorbance and transmittance is presented in Figure 14. As the dispersibility of nano-ZnO particles decreased, the absorbance and transmittance of the nanocomposite films displayed increase and decrease in the NIR range, respectively, suggesting that the absorbance and transmittance of NIR was probably related to the particle size, not to the nano-effect.

CONCLUSIONS

Poly(styrene butylacrylate) latex / nano-ZnO composites were prepared by blending poly(styrene butylacrylate) latex with a water slurry of nano-ZnO particles. The composites were then investigated by TEM, an Instron testing machine, DMA and UV-VIS-NIR spectrophotometry. It was found that the dispersant with long chains and strong affinity groups to pigments favored enhancing the dispersibility of nano-ZnO particles, and increasing dispersing time could also lead to more homogeneous nanocomposites.

The tensile strength, UV and NIR shielding properties of the nanocomposite polymers increased, and the T_g first increased then decreased, with increasing nano-ZnO content. But different ZnO particles have different effects on the mechanical and optical properties of the composite polymers due to size effect, surface effect and quantum effect. The nanocomposite polymers embedded with nano-ZnO particles had much higher tensile strength than the corresponding composite polymers with micro-ZnO particles, but the polymers containing 100 nm ZnO had even higher tensile strength than those containing 60 nm ZnO due to surface group effect. ZnO particles of 60 nm could more effectively shield UV rays than 100 nm ZnO particles, while micro-ZnO particles basically had no effect on the UV absorbance of the composite polymers. A blue-shift phenomenon was observed at 365 nm for nano-ZnO in the nanocomposite polymers. All of the composites with ZnO particles showed the NIR shielding property, but the NIR shielding property is related to particle size.

References

1. Takai, M.; Futsuhara, G.; Shimizu, C. P.; Lungu, J.; Nozue, Thin Solid Films 1998, 318, 117.
2. Xu, J. Q.; Pan, Q. Y.; Shun, Y. A.; Tian, Z. Z. Sensors and Actuators 2002, B66, 227.
3. Lou, X. J. Sens Trans Technol 1991, 3, 1.
4. Dong, L. F.; Cui, Z. L.; Zhang, Z. K. Nanostructure Material 1997, 8(7), 815.
5. Van Dijken, A.; Miulenkamp, E. A.; Vanmaekelbergh, D.; Meijerink, A. J Luminescence 2000, 90, 123.
6. Vanheusden, K.; Warren, W. L.; Seager, C. H.; Tallant, D. R.; Voigt, J. A.; Gnade, B. E. J Appl Phys 1996, 79(1), 7983.
7. Jose, J.; Abdul Khadar, M. Nanostructure Material 1999, 11(8), 1091.
8. Nan, C.-W.; Holten, S.; Birringer, R.; Gao, H.; Kliem, H.; Gleiter, H. Phys Stat Sol (A) 1997, 164, R1.
9. Lee, J.; Hwang, J. H.; Mashek, J. J.; Mason, T. O.; Miller, A. E.; Siegel, R. W.; J Mater Res 1995, 10, 2295.
10. Li, J. F.; Yao, L. Z.; Ye, C. H.; Mo, C. M.; Cai, W. L.; Zhang, Y. L.; Zhang, D. J Crystal Growth 2001, 223, 535.
11. Liu, Y. X.; Liu, Y. C.; Shen, D. Z.; Zhang, G. Z.; Fan, X. W.; Kong, X. G.; Mu, R. Solid State Comm 2002, 121, 531.
12. Wu, R.; Xie, C. S.; Xia, H.; Hu, J. H.; Wang, A. H. J Crystal Growth 2000, 217, 274.
13. Li, R. X.; Yabe, S.; Yamashita, M.; Momose, S.; Yoshida, S.; Yin, S.; Sato, T. Mater Chem Phys 2002, 75, 39.
14. Xiong, M. N.; Wu, L. M.; Zhou, S. X.; You, B. Polym Int 2002, 51, 1.
15. Fujihara, S.; Naito, H.; Kimura, T. Thin Solid Films 2001, 389, 227.
16. Vanheusden, K.; Seager, C. H.; Warren, W. L.; Tallant, D. R.; Viogt, J. A. Appl Phys Lett 1996, 68, 403.
17. Nyffenegger, R. M.; Craft, B.; Shaaban, M.; Gorer, S.; Erley, G.; Penner, R. M. Chem Mater 1998, 10, 1120.
18. Wang, Y.; N. Herron, J Phys Chem 1991, 95, 525.
19. Feng, X.; Zhu, X X. Appl Thermal Engineering 1997, 17, 249.